Control Design of the Quadrotor Aircraft based on the Integral Adaptive Improved Integral Backstepping Sliding Mode Scheme

Zhang Jinlong
School of Electrical Engineering and Automation, Jiangxi University of Science and Technology, Ganzhou 341000, China
2294477940@qq.com

Wang Jianhong
School of Electrical Engineering and Automation, Jiangxi University of Science and Technology, Ganzhou 341000, China | School of Engineering and Sciences, Tecnologico de Monterrey, Monterrey, 64849, Mexico
wangjianhong@nuaa.edu.cn

Wen Ruchun
School of Electrical Engineering and Automation, Jiangxi University of Science and Technology, Ganzhou 341000, China
9120180007@jxust.edu.cn

Luo Xi
School of Electrical Engineering and Automation, Jiangxi University of Science and Technology, Ganzhou 341000, China
3396297201@qq.com

Ding Yongjun
School of Electrical Engineering and Automation, Jiangxi University of Science and Technology, Ganzhou 341000, China
dingyongjun1021@163.com

Ahmad Taher Azar
College of Computer and Information Sciences, Prince Sultan University, Riyadh, Saudi Arabia | Automated Systems and Soft Computing Lab (ASSCL), Prince Sultan University, Riyadh, Saudi Arabia | Faculty of Computers and Artificial Intelligence, Benha University, Benha, Egypt
aazar@psu.edu.sa

Saim Ahmed
College of Computer and Information Sciences, Prince Sultan University, Riyadh, Saudi Arabia | Automated Systems and Soft Computing Lab (ASSCL), Prince Sultan University, Riyadh, Saudi Arabia
sahmed@psu.edu.sa

Ibrahim A. Hameed
Faculty of Science and Technology, Norwegian University of Life Science (NMBU), Trondheim, Norway
brahim.abdelhameed@nmbu.no

Ali Mahdi Zalzala
Department of Electronics and Communication Engineering, Uruk University, Baghdad 10001, Iraq
a.zalzala@uruk.edu.iq

Ibraheem Kasim Ibraheem
Department of Electrical Engineering, College of Engineering, University of Baghdad, Baghdad 10001, Iraq
ibraheemki@coeng.uobaghdad.edu.iq (corresponding author)

Received: 11 July 2024 | Revised: 9 August 2024 | Accepted: 22 August 2024

ABSTRACT

It is known that disturbances reduce tracking accuracy and control effect. To address these issues, in this paper, the Integral Adaptive Improved Integral Backstepping Sliding Mode Control (IAIIBSMC) method for position control of the quadrotor with uncertain disturbances, is proposed. Integrals are introduced into the adaptive reaching law and are extended to the control of virtual variables based on integral backstepping control, enhancing the system's anti-disturbance performance. The final combination with Sliding Mode Control (SMC) further improves system performance. Compared to the traditional Adaptive Integral Backstepping Control (AIBC), the proposed IAIIBSMC demonstrates superior tracking control, faster response, stronger anti-interference ability, and smaller overshoot. Experimental comparisons of different control methods and disturbances during fixed-point hovering and trajectory tracking show that the IAIIBSMC achieves better control. Specifically, the maximum position tracking error using IAIIBSMC is approximately 0.191 m, 22.04% lower than that of the AIBC. The steady-state error of IAIIBSMC is about 3 mm, which is negligible within the allowable range. These results validate the effectiveness and superiority of the proposed controller in achieving precise control under various disturbance conditions.

Keywords-quadrotor aircraft; integral backstepping sliding mode control; adaptive control; hovering control; trajectory tracking control

I. INTRODUCTION

In recent years, quadrotor aircrafts have found extensive applications in various fields thanks to their simple structure, convenient control, low cost, and easy production. These fields include aerial photography, monitoring, law enforcement, mapping, search and rescue, and more. The versatility of quadrotor aircrafts in these tasks underscores the importance of our research in improving their control systems [1-3].

Quadrotor aircraft control systems are complex, underdriven, nonlinear systems. The actual flight process is often subject to various external disturbances and structural and parametric uncertainties. The system's control performance and disturbance resistance were improved in [4-6]. There are many researchers that use linear and nonlinear control methods for quadrotor control design [7-22]. However, the performance of the linear controller is poor when the system deviates from its working state. Backstepping control in nonlinear control methods can effectively deal with the control problem of quadrotor cascade structures, with the disadvantage of poor robustness to disturbances [23-25]. The controller is designed to improve the system's robustness by combining the backstepping method with the Sliding Mode Control (SMC), although the latter suffers from tremor phenomena [26-28]. In [29], the Integral Backstepping SMC (IBSMC) with saturation function was proposed to reduce tremor. However, these controllers rely on knowledge of upper-bound perturbation, which is difficult to obtain in practice. Adaptive control has been widely used because it can adapt to and estimate the parameter changes of the system [30]. In [31], adaptive control is introduced, and an adaptive backstepping controller is designed. Then, compared with the integral terminal sliding mode and the traditional backstepping method, the tracking effect of the adaptive backstepping method is better. In [32], Adaptive Integral Backstepping Control (AIBC) is proposed to estimate the variable parameters of the system. The experimental results proved the method's effectiveness compared with the conventional integral backstepping controller, both with and without disturbances. In [33], the Adaptive Integral Backstepping SMC (AIBSMC) controller is proposed to implement quadrotor trajectory tracking, where the SMC uses a fast terminal sliding mode. The controller is stabilized in finite time while the tracking error converges within a neighborhood of the origin.

The above works do not consider further control of virtual variables in the backstepping design process. Therefore, this paper extends the integral to the virtual variables based on the traditional integral backstepping control and applies the idea of adaptive control to improve the adaptive convergence law. The Integral Adaptive Improved Integral Backstepping SMC (IAIIBSMC) method is proposed for controlling the quadrotor aircraft.

The main contributions of the current paper compared to the above literature are:

- Various uncertainties and neglected minor terms of the system are uniformly regarded as disturbances, and adaptive control is combined with integral backstepping

SMC, improving the system's robustness and immunity to disturbances.

- Extending the integral to the virtual variable improves the system's control performance by enhancing the integral backstepping control.
- The IAIIBSMC method was used to design the controller. The controller's stability was proved theoretically, the quadrotor fixed-point hovering and trajectory tracking control were realized, and the algorithm's effectiveness and feasibility were verified by simulation.
- Simulation of the model when subjected to various disturbances and comparison with the AIBC, Integral Adaptive Integral Backstepping Control (IAIBC), Integral Adaptive Improved Integral Backstepping Control (IAIIBC), and IAIIBSMC methods were conducted, IAIIBSMC exhibited better control effect and anti-disturbance ability.

II. QUADROTOR MODEL

The quadrotor can be seen in Figure 1. Its position and attitude are described by the ground coordinate system $E(OXYZ)$ and body coordinate system B($Oxyz$), respectively. where ϕ is the roll angle, θ is the pitch angle, ψ is the yaw angle, and R is the transformation matrix [1].

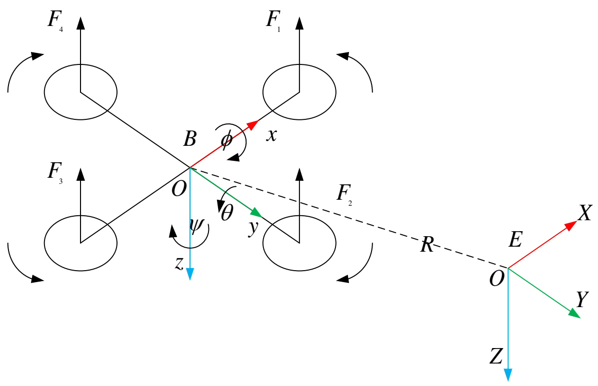

Fig. 1. Body coordinate system B and ground coordinate system E.

The quadrotor aircraft model was established after the following assumptions.

- **Assumption 1.** The body is rigid with a symmetrical structure, constant mass, and uniform distribution.
- **Assumption 2.** The ground coordinate system is inertial, and the body coordinate system's origin is the body's geometric center.
- **Assumption 3.** The force generated by each rotor is proportional to the square of the rotational speed.
- **Assumption 4.** The vertical distance from the center of the rotor to the center of mass of the body and the gyroscopic effect of the rotor were Ignored.

Under these assumptions, Newton's law and the moment of momentum theorem can obtain the simplified dynamic model of the quadrotor aircraft. The uncertainty of the quadrotor modeling and the neglected small terms and external disturbances are unified as disturbance D. The final simplified model of the quadrotor system is formulated as:

$$\begin{cases} \ddot{x} = -(\cos\phi\sin\theta\cos\psi + \sin\phi\sin\psi)\frac{1}{m}U_1 + D_x \\ \ddot{y} = -(\cos\phi\sin\theta\sin\psi - \sin\phi\cos\psi)\frac{1}{m}U_1 + D_y \\ \ddot{z} = g - (\cos\phi\cos\theta)\frac{1}{m}U_1 + D_z \\ \ddot{\phi} = \dot{\theta}\dot{\psi}(\frac{I_y - I_z}{I_x}) + \frac{l}{I_x}U_2 + D_\phi \\ \ddot{\theta} = \dot{\phi}\dot{\psi}(\frac{I_z - I_x}{I_y}) + \frac{l}{I_y}U_3 + D_\theta \\ \ddot{\psi} = \dot{\phi}\dot{\theta}(\frac{I_x - I_y}{I_z}) + \frac{1}{I_z}U_4 + D_\psi \end{cases} \tag{1}$$

$$\begin{cases} U_1 = k_t(\Omega_1^2 + \Omega_2^2 + \Omega_3^2 + \Omega_4^2) \\ U_2 = k_t(\Omega_4^2 - \Omega_2^2) \\ U_3 = k_t(\Omega_1^2 - \Omega_3^2) \\ U_4 = k_d(\Omega_1^2 + \Omega_3^2 - \Omega_2^2 - \Omega_4^2) \end{cases} \tag{2}$$

$$\begin{cases} a_1 = \frac{I_y - I_z}{I_x}, \quad b_1 = \frac{l}{I_x} \\ a_2 = \frac{I_z - I_x}{I_y}, \quad b_2 = \frac{l}{I_y} \\ a_3 = \frac{I_x - I_y}{I_z}, \quad b_3 = \frac{1}{I_z} \\ u_x = -(\cos\phi\sin\theta\cos\psi + \sin\phi\sin\psi) \\ u_y = -(\cos\phi\sin\theta\sin\psi - \sin\phi\cos\psi) \end{cases} \tag{3}$$

where Ω_i (i= 1,2,3,4) is the rotation speed of the four rotors, U_1 ~ U_4 represent the vertical input control quantity, the roll input control quantity, the pitch control input quantity, and the yaw input control quantity, respectively, k_t is the lift coefficient of the rotor, k_d is the drag torque coefficient of the rotor, and g is the acceleration of gravity.

Equation (1) and (3) yield:

$$\begin{cases} \dot{x}_1 = x_2 \\ \dot{x}_2 = \frac{u_x}{m}U_1 + D_x \\ \dot{x}_3 = x_4 \\ \dot{x}_4 = \frac{u_y}{m}U_1 + D_y \\ \dot{x}_5 = x_6 \\ \dot{x}_6 = g - \cos x_7 \cos x_9 \frac{1}{m}U_1 + D_z \\ \dot{x}_7 = x_8 \\ \dot{x}_8 = a_1 x_{10} x_{12} + b_1 U_2 + D_\phi \\ \dot{x}_9 = x_{10} \\ \dot{x}_{10} = a_2 x_8 x_{12} + b_2 U_3 + D_\theta \\ \dot{x}_{11} = x_{12} \\ \dot{x}_{12} = a_3 x_8 x_{10} + b_3 U_4 + D_\psi \end{cases} \tag{4}$$

where $x_1 = x$, $x_2 = \dot{x}$, $x_3 = y$, $x_4 = \dot{y}$, $x_5 = z$, $x_6 = \dot{z}$, $x_7 = \phi$, $x_8 = \dot{\phi}$, $x_9 = \theta$, $x_{10} = \dot{\theta}$, $x_{11} = \psi$, $x_{12} = \dot{\psi}$.

III. DESIGN OF THE INTEGRAL ADAPTIVE IMPROVED INTEGRAL BACKSTEPPING SLIDING MODE CONTROLLER

A. Structure of the Control System

The quadrotor control system structure is shown in Figure 2, which adopts a dual-loop control structure in which the inner loop controls the attitude, and the outer loop controls the position.

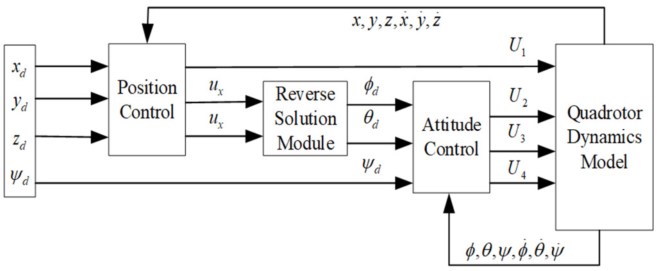

Fig. 2. Quadrotor aircraft control system structure.

B. Controller Design

Next, the controller of the quadrotor aircraft is designed. The state equation is introduced according to (4):

$$\begin{cases}\dot{x}_i = x_{i+1}, (i = 1,3,5,7,9,11)\\ \dot{x}_{i+1} = f(x) + g(x)u + d\end{cases} \tag{5}$$

where d is the interference. Let the expected value of x_i be x_{id}. The error variable is defined by:

$$z_i = x_i - x_{id} \tag{6}$$

There is:

$$\dot{z}_i = \dot{x}_i - \dot{x}_{id} = x_{i+1} - \dot{x}_{id} = z_{i+1} + \alpha_i + f_i \tag{7}$$

where $z_{i+1} = x_{i+1} - \alpha_i$ is the error variable, and α_i is the virtual control variable to be determined.

Let:

$$e_i(t) = \int_0^t z_i(\tau)\,d\tau \tag{8}$$

The selected Lyapunov function is:

$$V_1 = \frac{1}{2}z_i^2 + \frac{1}{2}\lambda_i e_i^2 \tag{9}$$

where $\lambda_i > 0$, and then:

$$\dot{V}_1 = z_i\dot{z}_i + \lambda_i e_i\dot{e}_i = z_i(\dot{z}_i + \lambda_i e_i) \tag{10}$$

$$= z_i(z_{i+1} + \alpha_i + f_i + \lambda_i e_i) \tag{11}$$

Take:

$$\alpha_i = -c_i z_i - \lambda_i e_i - f_i \tag{12}$$

Then:

$$\dot{V}_1 = -c_i z_i^2 + z_i z_{i+1} \tag{13}$$

where $c_i > 0$. Other variables are:

$$f_i = \dot{z}_i - x_{i+1} = -\dot{x}_{id}$$
$$\alpha_i = -c_i z_i - \lambda_i e_i - f_i = c_i z_i - \lambda_i e_i + \dot{x}_{id}$$
$$z_{i+1} = x_{i+1} - \alpha_i = c_i z_i + \dot{z}_i + \lambda_i e_i$$
$$= -\dot{x}_{id} + c_i z_i + \lambda_i e_i + x_{i+1}$$

The derivative of z_{i+1} is:

$$\begin{aligned}\dot{z}_{i+1} &= -\ddot{x}_{id} + c_i\dot{z}_i + \lambda_i z_i + \dot{x}_{i+1}\\ \alpha_i &= -\ddot{x}_{id} + c_i\dot{z}_i + f(x) + g(x)u + d\end{aligned} \tag{14}$$

Let:

$$e_{i+1}(t) = \int_0^t z_{i+1}(\tau)\,d\tau \tag{15}$$

The Lyapunov function is selected as:

$$V_2 = V_1 + \frac{1}{2}z_{i+1}^2 + \frac{1}{2}\lambda_{i+1}e_{i+1}^2 \tag{16}$$

where $\lambda_{i+1} > 0$. Then:

$$\begin{aligned}\dot{V}_1 &= -c_i z_i^2 + z_i z_{i+1} + z_{i+1}\dot{z}_{i+1} + \lambda_{i+1}e_{i+1}z_{i+1}\\ &= -c_i z_i^2 + z_{i+1}(z_i + \dot{z}_{i+1} + \lambda_{i+1}e_{i+1})\end{aligned} \tag{17}$$

If not combined with SMC, then take:

$$z_i + \dot{z}_{i+1} + \lambda_{i+1}e_{i+1} = -c_{i+1}z_{i+1}$$

If combined with SMC, the sliding mode surface is defined by:

$$s = z_{i+1} \tag{18}$$

To reduce the tremor, the saturation function is used to replace the traditional sign function:

$$z_i + \dot{z}_{i+1} + \lambda_{i+1}e_{i+1} = -\varepsilon sat(z_{i+1}) - kz_{i+1} \tag{19}$$

where $\varepsilon > 0$, $k > 0$.

The saturation function is:

$$sat(s) = \begin{cases}1 & s > \Delta\\ ks & |s| \le \Delta \quad k = \frac{1}{\Delta}\\ -1 & s < -\Delta\end{cases} \tag{20}$$

where $\Delta = 0.05$ and $k = 20$.

From (17)-(20), we can get:

$$\dot{V}_2 = -c_i z_i^2 - \varepsilon z_{i+1}sat(z_{i+1}) - kz_{i+1}^2 < 0 \tag{21}$$

From (14)-(19) we can get:

$$\begin{aligned}\dot{x}_{i+1} &= \ddot{x}_{id} - (1 + \lambda_i)z_i - c_i\dot{z}_i - \lambda_{i+1}e_{i+1}\\ &-\epsilon\, sat(z_{i+1}) - kz_{i+1}\end{aligned} \tag{22}$$

The control law is:

$$u = \frac{1}{g(x)}[\ddot{x}_{id} - (1 + \lambda_i)z_i - c_i\dot{z}_i - \lambda_{i+1}e_{i+1} - sat(z_{i+1}) - kz_{i+1} - f - d] \tag{23}$$

Since d is unknown, let the d estimate be $\hat{d}$, and the estimation error be defined by: $\tilde{d} = d - \hat{d}$.

Let:

$$K = \int_0^t \tilde{d}(\tau)\,d\tau \tag{24}$$

Changing d into $\hat{d}$ in (23), and then substituting it into (17), we obtain:

$$\dot{V}_2 = -c_i z_i^2 - \varepsilon z_{i+1} sat(z_{i+1}) - k z_{i+1}^2 + z_{i+1}\tilde{d} \quad (25)$$

Therefore, a new Lyapunov function is constructed as:

$$V = V_2 + \frac{1}{2\gamma}\tilde{d}^2 + \frac{1}{2}\beta K^2 \quad (26)$$

Then:

$$\dot{V} = -c_i z_i^2 - \varepsilon z_{i+1} sat(z_{i+1}) - k z_{i+1}^2 + \tilde{d}\left(z_{i+1} - \frac{1}{\gamma}\dot{\hat{d}} + \beta K\right) \quad (27)$$

where $\lambda_i > 0, \beta > 0$.

If selected:

$$\dot{\hat{d}} = \gamma(z_{i+1} + \beta K)$$

Then:

$$\dot{V} = -c_i z_i^2 - \varepsilon z_{i+1} sat(z_{i+1}) - k z_{i+1}^2 < 0 \quad (28)$$

At this time, the system is stable.

The control law and the adaptive reaching law of the IAIIBSMC method are:

$$\begin{cases} u = \frac{1}{g(x)}[\ddot{x}_{id} - (1+\lambda_i)z_i - c_i\dot{z}_i - \lambda_{i+1}e_{i+1} \\ \qquad -\varepsilon sat(z_{i+1}) - k z_{i+1} - f - \hat{d}] \\ \dot{\hat{d}} = \gamma(z_{i+1} + \beta K) \end{cases} \quad (29)$$

The control law and the adaptive reaching law of the IAIIBC method are:

$$\begin{cases} u = \frac{1}{g(x)}[\ddot{x}_{id} - (1+\lambda_i + c_i c_{i+1})z_i - (c_i + c_{i+1})\dot{z}_i \\ \qquad -\lambda_i c_{i+1} e_i - \lambda_{i+1}e_{i+1} - f - \hat{d}] \\ \dot{\hat{d}} = \gamma(z_{i+1} + \beta K) \end{cases} \quad (30)$$

The control law and the adaptive reaching law of the IAIBC method are:

$$\begin{cases} u = \frac{1}{g(x)}[\ddot{x}_{id} - (1+\lambda_i + c_i c_{i+1})z_i - (c_i + c_{i+1})\dot{z}_i \\ \qquad -\lambda_i c_{i+1} e_i - f - \hat{d}] \\ \dot{\hat{d}} = \gamma(z_{i+1} + \beta K) \end{cases} \quad (31)$$

The control law and the adaptive reaching law of the AIBC method are:

$$\begin{cases} u = \frac{1}{g(x)}[\ddot{x}_{id} - (1+\lambda_i + c_i c_{i+1})z_i - (c_i + c_{i+1})\dot{z}_i \\ \qquad -\lambda_i c_{i+1} e_i - f - \hat{d}] \\ \dot{\hat{d}} = \gamma z_{i+1} \end{cases} \quad (32)$$

Finally, according to (5), (6), and (29), identically, the control law and the adaptive reaching law for the quadrotor using the IAIIBSMC method to design the controller are:

Position x:

$$\begin{cases} u_x = \frac{m}{U_1}[\ddot{x}_d - (1+\lambda_1)z_1 - c_1\dot{z}_1 - \lambda_2 e_2 \\ \qquad -\varepsilon_1 sat(z_2) - k_1 z_2 - \hat{D}_x] \\ \qquad \dot{\hat{D}}_x = \gamma_1(z_2 + \beta_1 K_x) \\ z_1 = x - x_d, z_2 = c_1 z_1 + \dot{z}_1 + \lambda_1 e_1 \end{cases} \quad (33)$$

Position y:

$$\begin{cases} u_y = \frac{m}{U_1}[\ddot{y}_d - (1+\lambda_3)z_3 - c_3\dot{z}_3 - \lambda_4 e_4 \\ \qquad -\varepsilon_2 sat(z_4) - k_2 z_4 - \hat{D}_y] \\ \qquad \dot{\hat{D}}_y = \gamma_2(z_4 + \beta_2 K_y) \\ z_3 = y - y_d, z_4 = c_3 z_3 + \dot{z}_3 + \lambda_3 e_3 \end{cases} \quad (34)$$

Position z :

$$\begin{cases} U_1 = -\frac{m}{\cos\phi\cos\theta}[\ddot{z}_d - (1+\lambda_5)z_5 - c_5\dot{z}_5 \\ \quad -\lambda_6 e_6 - \varepsilon_3 sat(z_6) - k_3 z_6 - g - \hat{D}_z] \\ \qquad \dot{\hat{D}}_z = \gamma_3(z_6 + \beta_3 K_z) \\ z_5 = z - z_d, z_6 = c_5 z_5 + \dot{z}_5 + \lambda_5 e_5 \end{cases} \quad (35)$$

Roll angle ϕ:

$$\begin{cases} U_2 = \frac{1}{b_1}[\ddot{\phi}_d - (1+\lambda_7)z_7 - c_7\dot{z}_7 - \lambda_8 e_8 \\ \quad -\varepsilon_4 sat(z_8) - k_4 z_8 - a_1\dot{\theta}\dot{\psi} - \hat{D}_\phi] \\ \qquad \dot{\hat{D}}_\phi = \gamma_4(z_8 + \beta_4 K_\phi) \\ z_7 = \phi - \phi_d, z_8 = c_7 z_7 + \dot{z}_7 + \lambda_7 e_7 \end{cases} \quad (36)$$

Pitch angle θ:

$$\begin{cases} U_3 = \frac{1}{b_2}[\ddot{\theta}_d - (1+\lambda_9)z_9 - c_9\dot{z}_9 - \lambda_{10} e_{10} \\ \quad -\varepsilon_5 sat(z_{10}) - k_5 z_{10} - a_2\dot{\phi}\dot{\psi} - \hat{D}_\theta] \\ \qquad \dot{\hat{D}}_\theta = \gamma_5(z_{10} + \beta_5 K_\theta) \\ z_9 = \theta - \theta_d, z_{10} = c_9 z_9 + \dot{z}_9 + \lambda_9 e_9 \end{cases} \quad (37)$$

Yaw angle ψ :

$$\begin{cases} U_4 = \frac{1}{b_3}[\ddot{\psi}_d - (1+\lambda_{11})z_{11} - c_{11}\dot{z}_{11} - \lambda_{12} e_{12} \\ \quad -\varepsilon_6 sat(z_{12}) - k_6 z_{12} - a_3\dot{\phi}\dot{\theta} - \hat{D}_\psi] \\ \qquad \dot{\hat{D}}_\psi = \gamma_6(z_{12} + \beta_6 K_\psi) \\ z_{11} = \psi - \psi_d, z_{12} = c_{11} z_{11} + \dot{z}_{11} + \lambda_{11} e_{11} \end{cases} \quad (38)$$

IV. SIMULATION RESULTS

The IAIIBSMC controller was designed to simulate the quadrotor's fixed-point hovering and trajectory tracking. The parameters of the quadrotor model are shown in Table I. The controller parameters were simulated and debugged, as shown in Table II. If a parameter is not included, its value is zero to indicate it. In order to compare the control effects of different methods, the parameters of other methods were asigned the same values.

TABLE I. QUADROTOR MODEL PARAMETERS

Variable	Value
m	0.75 kg
l	0.25 m
k_t	7.5e^{-7} N.ms^2
k_d	7.5e^{-7} N.ms^2
I_x	19.688e^{-3} kg.m^2
I_y	19.681e^{-3} kg.m^2
I_z	3.983e^{-2} kg.m^2
g	9.8 m/s^2

TABLE II. CONTROLLER PARAMETERS

Control method	Hovering control parameters	Tracking control parameters
AIBC	$c_i = 1, c_{i+1} = 4$ $\lambda_i = 0.5, \lambda_{i+1} = 0$ $\gamma_j = 50, \beta_j = 0$	$c_i = 1, c_{i+1} = 1$ $\lambda_i = 0.5, \lambda_{i+1} = 0$ $\gamma_j = 50, \beta_j = 0$
IAIBC	$c_i = 1, c_{i+1} = 4$ $\lambda_i = 0.5, \lambda_{i+1} = 0$ $\gamma_j = 50$ $\beta_j = \frac{0.2}{\gamma_j}$	$c_i = 1, c_{i+1} = 1$ $\lambda_i = 0.5, \lambda_{i+1} = 0$ $\gamma_j = 50$ $\beta_j = \frac{0.2}{\gamma_j}$
IAIIBC	$c_i = 1, c_{i+1} = 4$ $\lambda_i = 0.5, \lambda_{i+1} = 5$ $\gamma_j = 50$ $\beta_j = \frac{0.2}{\gamma_j}$	$c_i = 1, c_{i+1} = 1$ $\lambda_i = 0.5, \lambda_{i+1} = 5$ $\gamma_j = 50$ $\beta_j = \frac{0.2}{\gamma_j}$
IAIIBSMC	$c_i = 1, c_{i+1} = 0$ $\lambda_i = 0.5, \lambda_{i+1} = 5$ $\gamma_j = 50$ $\beta_j = \frac{0.2}{\gamma_j}$ $\varepsilon_1, \varepsilon_2 = 3$ $k_1, k_2 = 1$ $\varepsilon_3, \varepsilon_4, \varepsilon_5, \varepsilon_6 = 4$ $k_3, k_4, k_5, k_6 = 20$	$c_i = 1, c_{i+1} = 0$ $\lambda_i = 0.5, \lambda_{i+1} = 5$ $\gamma_j = 50$ $\beta_j = \frac{0.2}{\gamma_j}$ $\varepsilon_j = 0.1, k_j = 1$

where $i = 1,3,5,7,9,11$, $j = 1,2,3,4,5,6$.

A. Fixed Point Hovering

The design of the position and attitude of the quadrotor is the same, so the control effect of the position and attitude is similar. Assuming that the initial state of the quadrotor is zero, it flies from the origin of the ground coordinate system (0,0,0) to the target coordinate (1,0,0) to remain hovering. Taking position x control as an example, six groups of experiments were designed for different D_x, and the control effect and anti-disturbance ability of AIBC, IAIBC, IAIIBC, and IAIIBSMC were compared. Let the initial interference be:

$$D_x = 5,\ \ D_y = 5,\ \ D_z = 5,$$
$$D_\phi = 3,\ \ D_\theta = 4,\ \ D_\psi = 5 \tag{39}$$

The first group is the case where the initial interference is constant, and there is no other interference during the flight, as shown in Figure 3. At this time, there is:

$$d_1 = 0, D_x = 5 + d_1 = 5 \tag{40}$$

The second group added a rectangular square wave with amplitude 1 and pulse width of 2 s to the system at 20 s to simulate other instantaneous disturbances during flight, as shown in Figure 4:

$$d_2 = \varepsilon(t-20) - \varepsilon(t-22),$$
$$D_x = 5 + d_2 = 5 + \varepsilon(t-20) - \varepsilon(t-22) \tag{41}$$

where $\varepsilon(t)$ is the unit step signal. The third group added a constant value disturbance with amplitude 5 to the system at 20 s to simulate the flight process with other constant value disturbances, as shown in Figure 5:

$$d_3 = 5\varepsilon(t-20),$$
$$D_x = 5 + d_3 = 5 + 5\varepsilon(t-20) \tag{42}$$

The fourth group added a sine wave with amplitude 1 and angular velocity 1 rad/s to the system during the whole process to simulate the situation of being subjected to sinusoidal continuous interference in actual flight, as shown in Figure 6:

$$d_4 = sin(t), D_x = 5 + d_4 = 5 + sin(t) \tag{43}$$

The fifth group added white noise $w(t)$ to the system in the whole process to verify the control effect of the quadrotor under white noise interference, as shown in Figure 7

$$d_5 = w(t), D_x = 5 + d_5 = 5 + w(t) \tag{44}$$

The sixth group superimposed the above interference to form a comprehensive interference to ensure that the simulation is more in line with the actual flight situation, as shown in Figure 8:

$$\begin{aligned} d_6 &= d_2 + d_3 + d_4 + d_5 \\ &= 6\varepsilon(t-20) - \varepsilon(t-22) + \sin(t) + w(t) \\ D_x &= 5 + d_6 \\ &= 5 + 6\varepsilon(t-20) - \varepsilon(t-22) + \sin(t) + w(t) \end{aligned} \tag{45}$$

The comprehensive interference d_6 is shown in Figure 9.

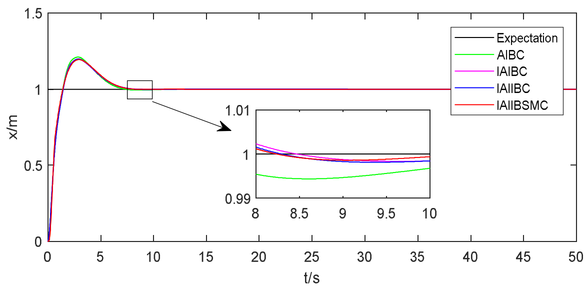

Fig. 3. Hovering control without other disturbances during flight.

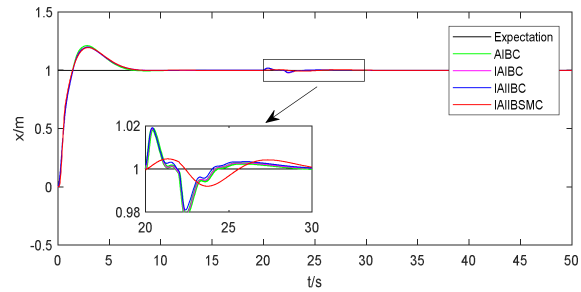

Fig. 4. Hovering control under instantaneous disturbances during flight.

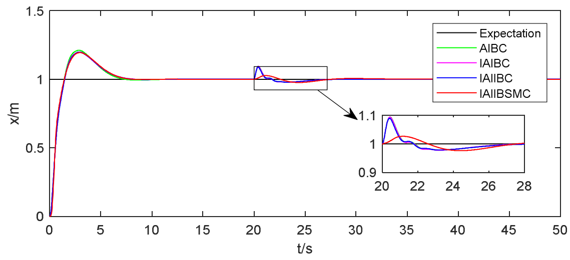

Fig. 5. Hovering control subject to constant disturbances during flight.

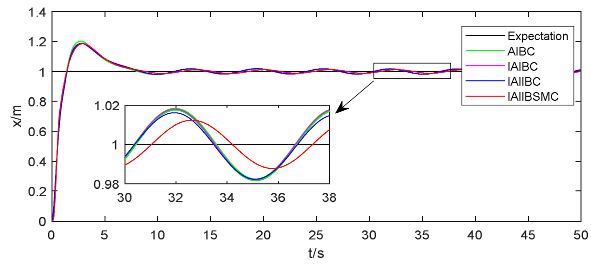

Fig. 6. Hovering control subject to sinusoidal continuous interference during flight.

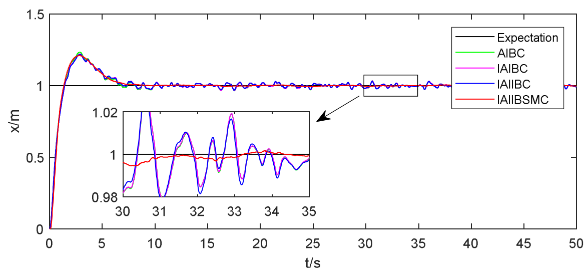

Fig. 7. Hovering control disturbed by white noise during flight.

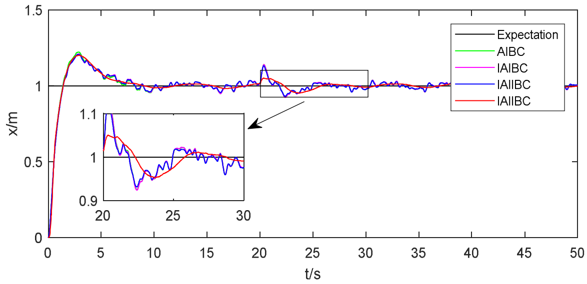

Fig. 8. Hovering control subject to comprehensive interference during flight.

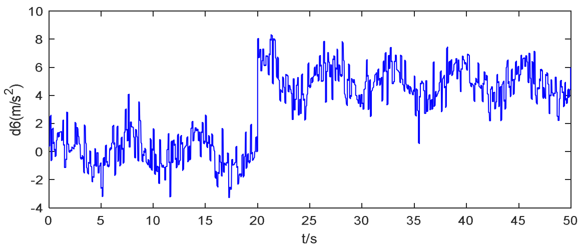

Fig. 9. Comprehensive interference curve.

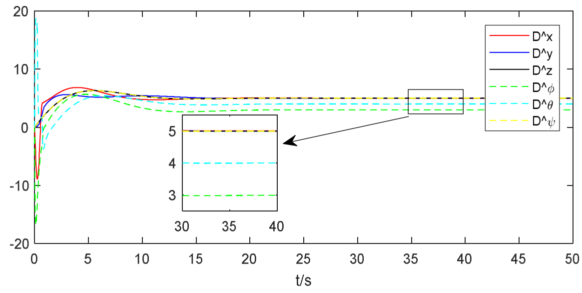

Fig. 10. Adaptive parameter update curve.

In order to compare the fluctuation of the quadrotor aircraft after being disturbed, the Mean Square Error (MSE) is as the fluctuation index of position x. The smaller the MSE value, the better. MSE is calculated by:

$$MSE = \frac{1}{N}\sum_{i=1}^{N}(x_i - \hat{x}_i)^2 \tag{46}$$

where N is the total number of samples, x_i is the i actual position, and $\hat{x}_i$ is the i expected position. The MSE of the quadrotor under various disturbances is shown in Table III. The calculation interval is (20,30).

TABLE III. MSE OF QUADROTOR AIRCRAFT UNDER VARIOUS DISTURBANCES DURING FLIGHT

Controller	**Instantaneous disturbance**	**Constant disturbance**	**Sine continuous disturbance**	**White noise interference**	**comprehensive interference**
AIBC	4.836e-5	5.392e-4	1.601e-4	1.407e-4	1.547e-3
IAIBC	4.780e-5	5.327e-4	1.590e-4	1.411e-4	1.534e-3
IAIIBC	4.161e-5	4.769e-4	1.348e-4	1.313e-4	1.344e-3
IAIIBSMC	1.648e-5	2.144e-4	7.806e-5	1.068e-5	1.091e-4
Interval	(20,30)	(20,30)	(20,30)	(20,30)	(20,30)

The fixed-point hovering simulation results are shown in Figures 3-8. The black curve is the expected curve, the green is the AIBC curve, the magenta is the IAIBC curve, the blue is the IAIIBC curve, and the red is the IAIIBSMC curve.

As shown in Figure 3, the interference remains unchanged during the quadrotor flight. The IAIIBSMC, IAIIBC, and IAIBC have smaller overshoot and shorter adjustment time than the traditional AIBC method, and the IAIIBSMC has the best control effect. Figure 10 shows the adaptive parameter update process of IAIIBSMC.

In Figures 4-6, instantaneous interference, constant interference, and sinusoidal continuous interference are added to the x direction during the flight. The system deviates from the equilibrium position and D_x is shown in (41)-(43). The Figutrd clearly show that the deviation of IAIIBSMC is the smallest, and its curve is smoother. According to Table III, IAIIBSMC has a better control effect than IAIIBC, IAIIBC has a better control effect than IAIBC, and IAIBC has a better control effect than AIBC.

As shown in Figure 7, white noise interference is added to the x direction during the flight and D_x is shown in (44). Combining Figure 7 and Table III, it can be seen that the control effect of IAIIBSMC is the best among the considered methods. The control effect of IAIIBC is slightly better than IAIBC and AIBC's. In comparison, the control effect of IAIBC is worse than that of AIBC, which indicates that the controller has different control effects on different disturbances.

In Figure 8, the system is subject to comprehensive interference and D_x is shown in (45). Combining Figure 8 and Table III, it can be seen that IAIIBSMC has the best control effect, more vital anti-interference ability, and smoother curve.

In summary, the IAIIBSMC method overperforms the traditional AIBC method. The reason is that IAIIBSMC treats the virtual variables based on AIBC, thus affecting the control of the actual variables while the adaptive reaching law is improved. The advantage of the improved adaptive reaching law is that the influence on the system decreases when the disturbance changes. The disadvantage is that the steady-state error will increase, but the enhanced steady-state error is still small compared to the tracking curve and can be ignored. Finally, SMC is added to improve the system's robustness and reduce the steady-state error. It can be seen from Table III that the minimum MSE of the quadrotor aircraft under various disturbances is acquired with the IAIIBSMC method, which indicates that the process has a good control effect on multiple forms of external disturbances and is more in line with the actual flight of the quadrotor.

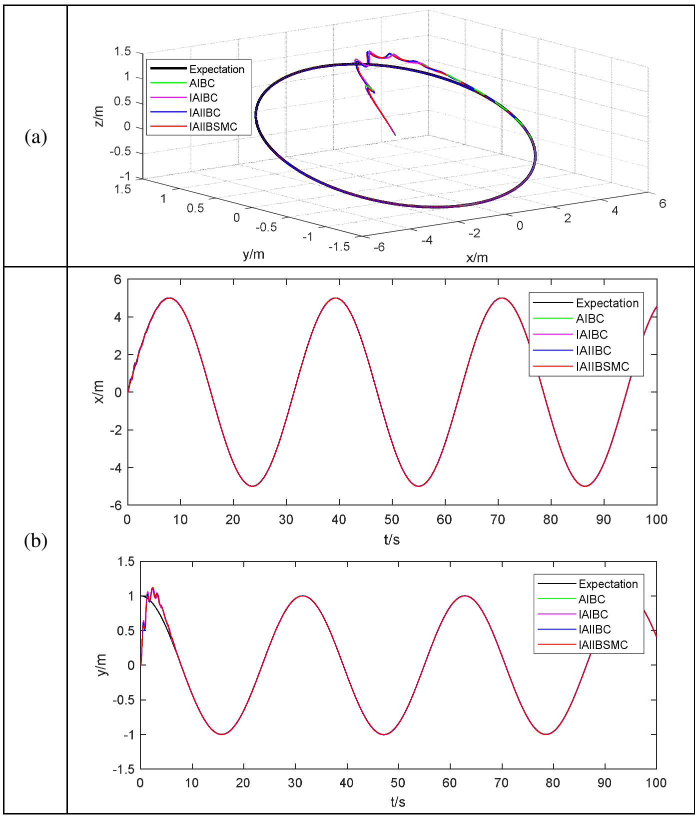

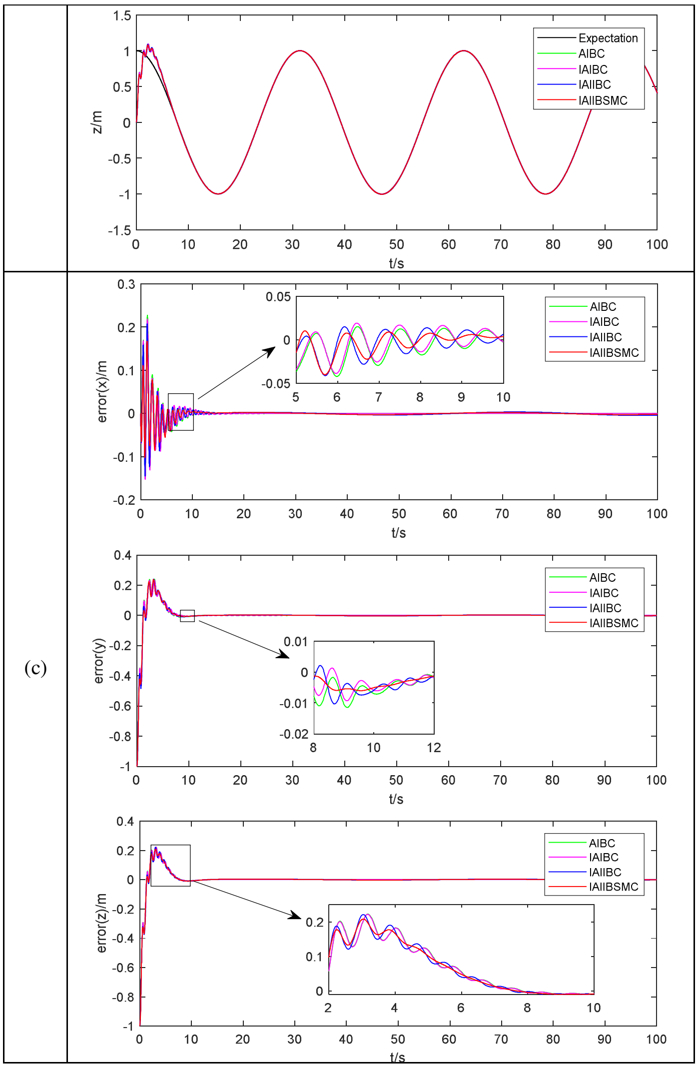

Fig. 11. Elliptic trajectory tracking without other interference during flight. (a) Three-dimensional trajectory, (b) position tracking curve, (c) position tracking error curve.

B. Trajectory Tracking

Ellipse and helix are chosen as the reference trajectories, the initial state of the quadrotor is set to zero, and the initial interference is shown in (39). The following is discussed in two cases. At first, when the quadrotor's initial interference is constant, several methods' control effects are compared and verified. Then, taking the position x control as an example, the trajectory tracking experiment is carried out by applying the comprehensive interference d_6 in the x direction of the quadrotor aircraft during the flight. The interference D_x from (45) shows the trajectory tracking and the control effects of AIBC, IAIBC, IAIIBC, and IAIIBSMC were verified and compared.

The ellipse reference trajectory is :

$$\begin{cases} x = 5\,sin(0.2t) \\ y = cos(0.2t) \\ z = cos(0.2t) \end{cases} \tag{47}$$

The spiral reference trajectory is:

$$\begin{cases} x = 5\,sin(0.2t) \\ y = cos(0.2t) \\ z = 0.2t \end{cases} \tag{48}$$

Figures 11 and 12 show the ellipse and spiral trajectory tracking simulation when there is no interference in the flight process. When the flight process is subjected to comprehensive interference in the x direction, the tracking simulation is shown in Figures 13 and 14.

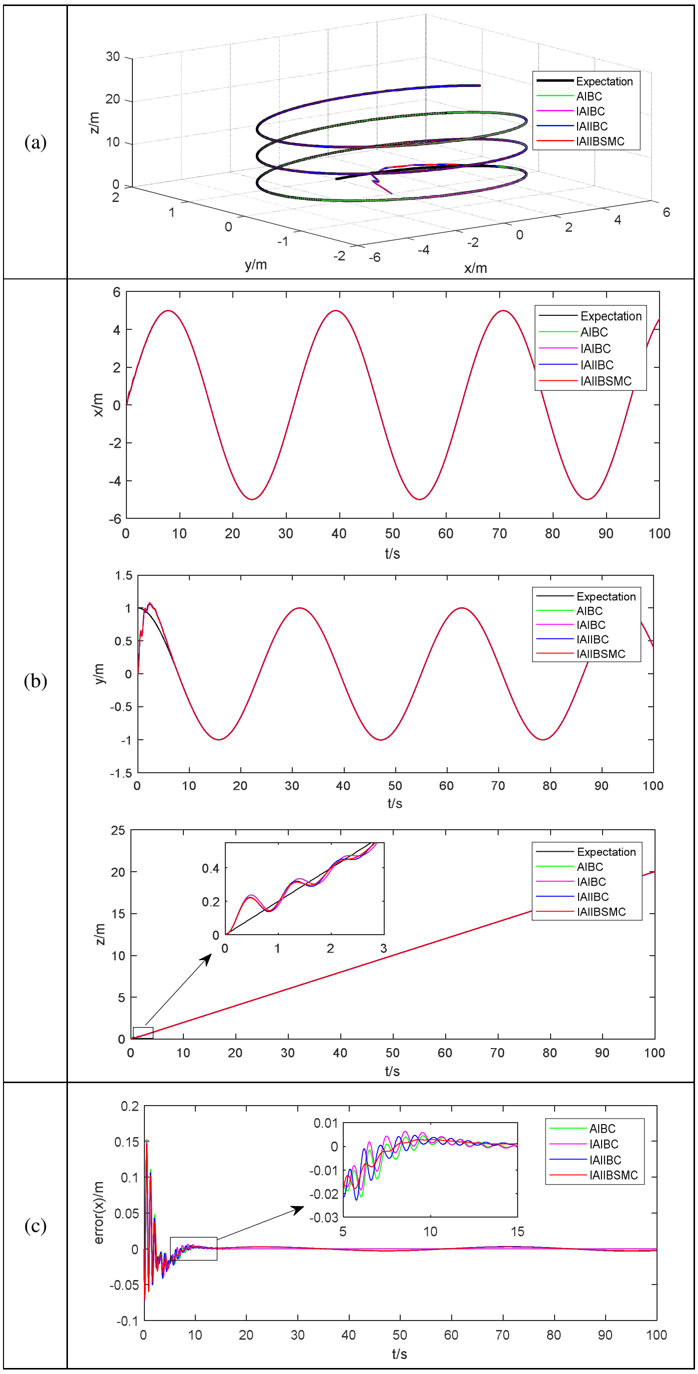

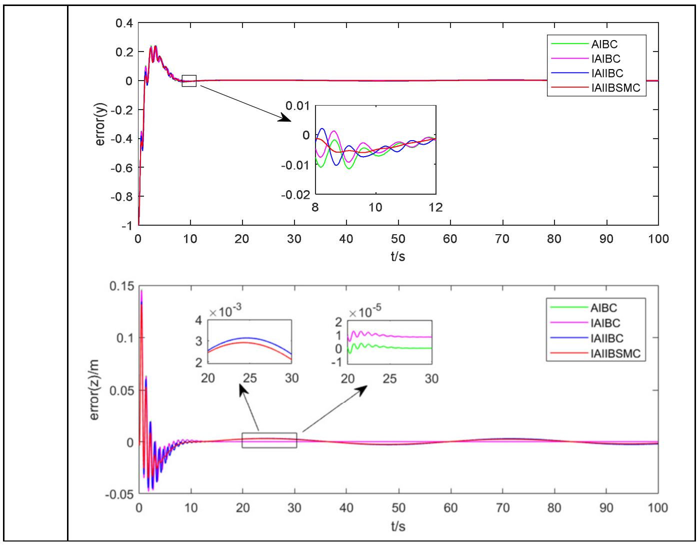

Fig. 12. Spiral trajectory tracking without other interference during flight. (a) Three-dimensional trajectory, (b) position tracking curve, (c) position tracking error curve.

Figures 11 and 12 show the flight process without other disturbances. The three-dimensional trajectory tracking of the ellipse and the spiral line is shown in Figures 11(a) and 12(a). It can be seen that these methods can control the quadrotor tracking ellipse and spiral line. As can be seen in Figures 11(b) and 12(b), the tracking curves of positions and the expected trajectories correspond to (47) and (48), respectively. The position tracking error curve in Figures 11(c) and 12(c) shows that the error will eventually tend to zero, while the overshoot of the IAIIB-SMC method is smaller, and the curve is smoother and more stable. However, the steady-state error is slightly larger than that of AIBC. In Figure 12(c), the steady-state error of the position tracking of IAIIBSMC is about 3 mm, and is negligible within the allowable range compared with the tracking curve.

Figures 13 and 14 show the tracking of the comprehensive interference in the x axis direction during flight. Figures 13(a) and 14(a) show the three-dimensional trajectory tracking of ellipse and spiral lines. The considered methods control the quadrotor tracking ellipse and spiral line, but the tracking control performance of AIBC is poor. As shown in Figures 13(b) and 14(b), which show the tracking curves of positions x, y, and z, the expected trajectories correspond to (47) and (48), respectively. Figures 13(c) and 14(c) show the position tracking error curves. D_x changes during flight, and the error(x) curves in Figures 13(c) and 14(c) eventually fluctuate up and down around zero. The change of D_x affects u_x and thus affects the roll angle ϕ. y is related to ϕ, so that the error (y) curve fluctuates up and down near 0. Compared to other methods, the error (x) and error (y) curves of the IAIIBSMC method are smoother, less volatile, and closer to zero. Taking the error (x) curve in Figure 13(c) as an example, the position x tracks the curve 5 sin (0.2t) m, the maximum error of IAIIBSMC is about 0.191 m, the maximum error of IAIIBC is about 0.227 m, the maximum error of IAIBC is about 0.237 m, and the maximum error of AIBC is about 0.245 m. The maximum error of IAIIBSMC is 22.04 % lower than that of AIBC.

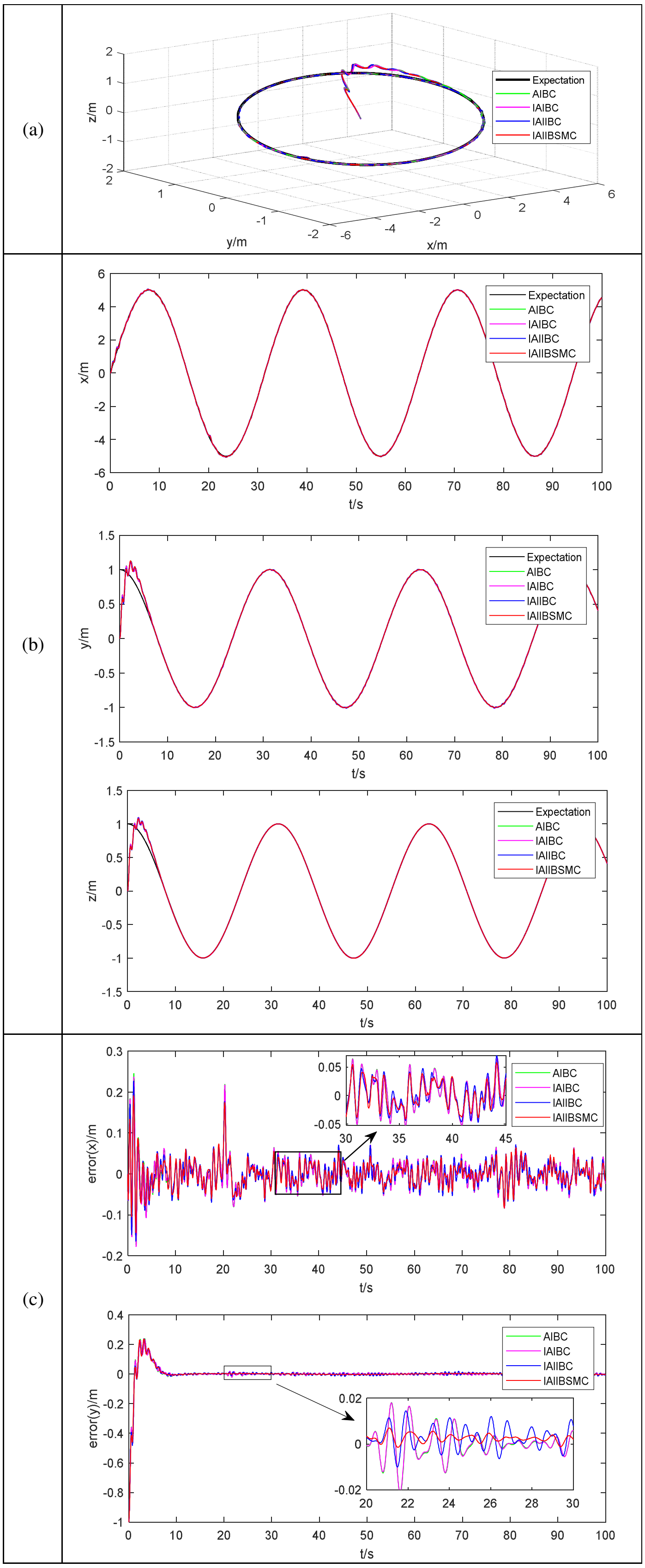

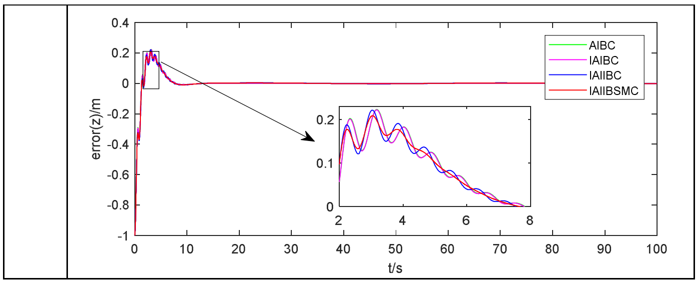

Fig. 13. Elliptic trajectory tracking under other comprehensive disturbances during flight. (a) Three-dimensional trajectory, (b) position tracking curve, (c) Position tracking error curve.

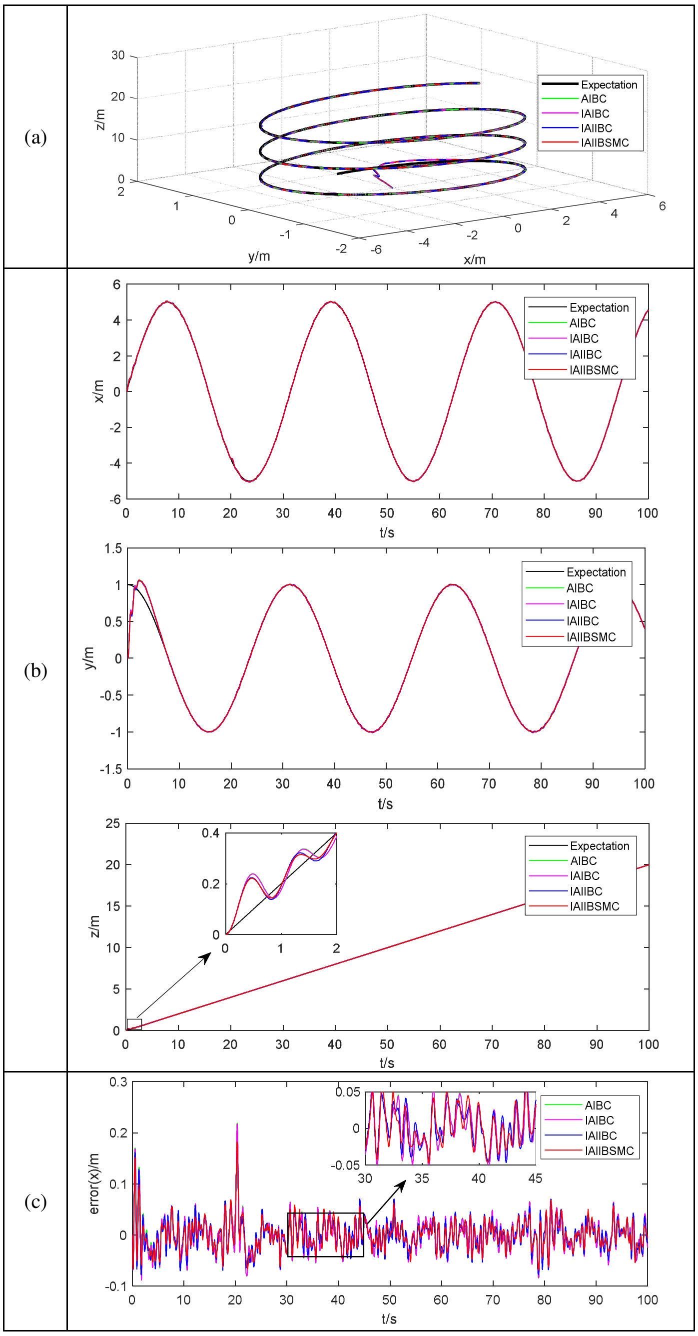

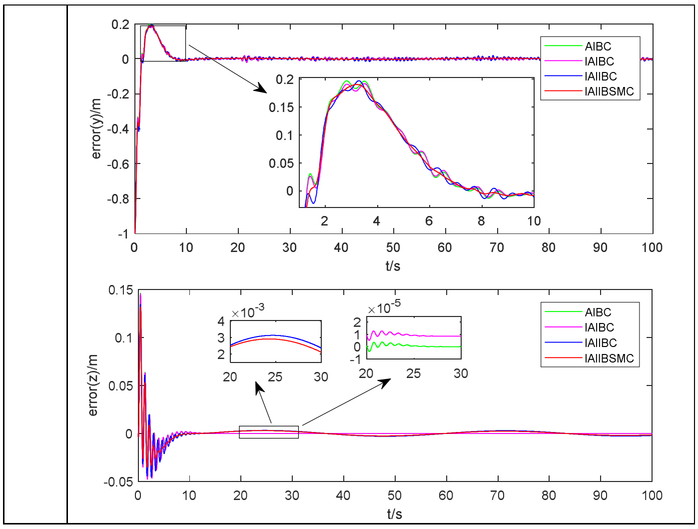

Fig. 14. Spiral trajectory tracking under other comprehensive disturbances during flight. (a) Three-dimensional trajectory, (b) position tracking curve, (c) Position tracking error curve.

The z-axis direction disturbance is unchanged, and error(z) will eventually converge to zero. IAIIBSMC has a slightly larger steady-state error than the AIBC method, the tracking steady-state error of IAIIBSMC is about 3 mm, as obtained from Figure 14(c), which is negligible compared to the tracking curves within the allowable range.

The proposed IAIIBSMC method introduces several innovations that enhance quadrotor control:

- Integration of Adaptive Control: The adaptive component allows the controller to adjust in real-time to changing conditions, improving robustness.
- Extended Integral Backstepping: The method significantly enhances the system's anti-disturbance capabilities by extending the integral term to virtual variables.
- SMC: This ensures robustness against model uncertainties and external disturbances, leading to more accurate tracking and stable flight.

The comparative analysis between IAIIBSMC and the traditional Adaptive Integral Backstepping Control (AIBC) method can be seen in Table IV. Key performance metrics were analyzed, including response time, maximum position error, and overshoot.

TABLE IV. COMPARISON ANALYSIS

Metric	IAIIBSMC	AIBC	Improvement (%)
Response time	2.5 s	3.0 s	16.7%
Max position error	0.191 m	0.245 m	22.04%
Overshoot	5%	7%	28.6%

The simulation results demonstrate the effectiveness of the proposed IAIIBSMC method. Key findings include:

- Faster Response Time: The IAIIBSMC method achieved a response time of 2.5 s, compared to the 3.0 s of the AIBC method, representing a 16.7% improvement.
- Reduced Position Error: The maximum position error using IAIIBSMC was 0.191 m, a 22.04% reduction compared to AIBC.
- Lower Overshoot: The IAIIBSMC method exhibited an overshoot of 5%, resulting in a 28.6% improvement.

In summary, the IAIIBSMC method has the best control effect in the control design of the quadrotor aircraft. The IAIIBAMC method has lower overshoot, faster response, stronger anti-disturbance ability, and faster stability than the traditional AIBC method. The interference of the quadrotor in real flight is unknown and complex. In reality, there is unknown and complex interference in all three positional directions of the quadrotor, so it is better to use IAIIBSMC to design the controller, which is more in line with the real situation.

V. CONCLUSION

In this paper, the IAIIBSMC method is proposed for controlling the virtual variables during the design process to influence the control effect of the actual variables. The adaptive convergence law is improved to enhance the system's immunity to interference. The system performance is further improved by combining it with the sliding-mode control, and stability analysis was performed on the design process of the method. Compared with the traditional AIBC method, the proposed IAIIBSMC method has a better control effect on various types of complex unknown disturbances that are more in line with the actual flight conditions. The simulation results show the effectiveness and superiority of the IAIIBSMC method. The simulation section underscores the significant improvements achieved by the proposed IAIIBSMC method, validating its effectiveness for precise quadrotor control in dynamic environments. The proposed method demonstrates a faster response, stronger anti-interference capability, and smaller overshoot compared to traditional methods, making it highly suitable for high-precision and reliability applications. In addition, parameter identification can be added on this basis to improve the system performance further and make the control effect more accurate and effective; similarly, further control analysis can be made for the system's state safety constraints.

ACKNOWLEDGMENT

The authors would like to acknowledge the support of Prince Sultan University, Riyadh, Saudi Arabia, in paying the Article Processing Charges (APC) of this publication. Special acknowledgment to Automated Systems and Soft Computing Lab (ASSCL), Prince Sultan University, Riyadh, Saudi Arabia.

REFERENCES

[1] M. Rinaldi, S. Primatesta, and G. Guglieri, "A Comparative Study for Control of Quadrotor UAVs," *Applied Sciences*, vol. 13, no. 6, Jan. 2023, Art. no. 3464, https://doi.org/10.3390/app13063464.

[2] G. Sonugur, "A Review of quadrotor UAV: Control and SLAM methodologies ranging from conventional to innovative approaches," *Robotics and Autonomous Systems*, vol. 161, Mar. 2023, Art. no. 104342, https://doi.org/10.1016/j.robot.2022.104342.

[3] S. I. Abdelmaksoud, M. Mailah, and A. M. Abdallah, "Control Strategies and Novel Techniques for Autonomous Rotorcraft Unmanned Aerial Vehicles: A Review," *IEEE Access*, vol. 8, pp. 195142–195169, Jan. 2020, https://doi.org/10.1109/ACCESS.2020.3031326.

[4] M. Idrissi, M. Salami, and F. Annaz, "A Review of Quadrotor Unmanned Aerial Vehicles: Applications, Architectural Design and Control Algorithms," *Journal of Intelligent & Robotic Systems*, vol. 104, no. 2, Jan. 2022, Art. no. 22, https://doi.org/10.1007/s10846-021-01527-7.

[5] W. Zhu, H. Du, Y. Cheng, and Z. Chu, "Hovering control for quadrotor aircraft based on finite-time control algorithm," *Nonlinear Dynamics*, vol. 88, no. 4, pp. 2359–2369, Jun. 2017, https://doi.org/10.1007/s11071-017-3382-8.

[6] G. E. M. Abro, V. S. Asirvadam, S. A. Bin Mohd Zulkifli, A. Sattar, D. Kumar, and A. Anwer, "Effects of unmodelled dynamic factors on an under-actuated quadrotor: A review of hybrid observer design methods," *Measurement and Control*, vol. 53, no. 9–10, pp. 1978–1987, Nov. 2020, https://doi.org/10.1177/0020294020964236.

[7] C. Rosales, S. Tosetti, C. Soria, and F. Rossomando, "Neural Adaptive PID Control of a Quadrotor using EFK," *IEEE Latin America Transactions*, vol. 16, no. 11, pp. 2722–2730, Nov. 2018, https://doi.org/10.1109/TLA.2018.8795113.

[8] S. Singh, A. T. Azar, A. Ouannas, Q. Zhu, W. Zhang, and J. Na, "Sliding mode control technique for multi-switching synchronization of chaotic systems," in *9th International Conference on Modelling, Identification and Control*, Kunming, China, Jul. 2017, pp. 880–885, https://doi.org/10.1109/ICMIC.2017.8321579.

[9] A. Sir Elkhatem and S. Naci Engin, "Robust LQR and LQR-PI control strategies based on adaptive weighting matrix selection for a UAV position and attitude tracking control," *Alexandria Engineering Journal*, vol. 61, no. 8, pp. 6275–6292, Aug. 2022, https://doi.org/10.1016/j.aej.2021.11.057.

[10] A. Aboudonia, A. El-Badawy, and R. Rashad, "Disturbance observer-based feedback linearization control of an unmanned quadrotor helicopter," *Proceedings of the Institution of Mechanical Engineers, Part I: Journal of Systems and Control Engineering*, vol. 230, no. 9, pp. 877–891, Oct. 2016, https://doi.org/10.1177/0959651816656951.

[11] T. S. Gorripotu, H. Samalla, Ch. Jagan Mohana Rao, A. T. Azar, and D. Pelusi, "TLBO Algorithm Optimized Fractional-Order PID Controller for AGC of Interconnected Power System," in *Soft Computing in Data Analytics*, J. Nayak, A. Abraham, B. M. Krishna, G. T. Chandra Sekhar, and A. K. Das, Eds. New York, NY, USA: Springer, 2019, pp. 847–855.

[12] K. Djamel, M. Abdellah, and A. Benallegue, "Attitude Optimal Backstepping Controller Based Quaternion for a UAV," *Mathematical Problems in Engineering*, vol. 2016, no. 1, 2016, Art. no. 8573235, https://doi.org/10.1155/2016/8573235.

[13] C. Xiu, F. Liu, and G. Xu, "General model and improved global sliding mode control of the four-rotor aircraft," *Proceedings of the Institution of Mechanical Engineers, Part I: Journal of Systems and Control Engineering*, vol. 232, no. 4, pp. 383–389, Apr. 2018, https://doi.org/10.1177/0959651817708066.

[14] S. Abdelmalek, A. T. Azar, and D. Dib, "A Novel Actuator Fault-tolerant Control Strategy of DFIG-based Wind Turbines Using Takagi-Sugeno Multiple Models," *International Journal of Control, Automation and Systems*, vol. 16, no. 3, pp. 1415–1424, Jun. 2018, https://doi.org/10.1007/s12555-017-0320-y.

[15] J. Yu, P. Shi, and L. Zhao, "Finite-time command filtered backstepping control for a class of nonlinear systems," *Automatica*, vol. 92, pp. 173–180, Jun. 2018, https://doi.org/10.1016/j.automatica.2018.03.033.

[16] C. Hua, G. Feng, and X. Guan, "Robust controller design of a class of nonlinear time delay systems via backstepping method," *Automatica*, vol. 44, no. 2, pp. 567–573, Feb. 2008, https://doi.org/10.1016/j.automatica.2007.06.008.

[17] T. Espinoza, A. E. Dzul, R. Lozano, and P. Parada, "Backstepping - Sliding Mode Controllers Applied to a Fixed-Wing UAV," *Journal of Intelligent & Robotic Systems*, vol. 73, no. 1, pp. 67–79, Jan. 2014, https://doi.org/10.1007/s10846-013-9955-y.

[18] R. Coban, "Backstepping Sliding Mode Tracking Controller Design and Experimental Application to an Electromechanical System," *Journal of Control Engineering and Applied Informatics*, vol. 19, no. 3, pp. 88–96, Sep. 2017, https://doi.org/10.61416/ceai.v19i3.4647.

[19] A. T. Azar and F. E. Serrano, "Stabilization and Control of Mechanical Systems with Backlash," in *Handbook of Research on Advanced Intelligent Control Engineering and Automation*, Hershey, PA, USA: IGI Global, 2015, pp. 1–60.

[20] F. Alotaibi, A. Al-Dhaqm, and Y. D. Al-Otaibi, "A Conceptual Digital Forensic Investigation Model Applicable to the Drone Forensics Field," *Engineering, Technology & Applied Science Research*, vol. 13, no. 5, pp. 11608–11615, Oct. 2023, https://doi.org/10.48084/etasr.6195.

[21] A. Hashmi, "A Novel Drone-based Search and Rescue System using Bluetooth Low Energy Technology," *Engineering, Technology & Applied Science Research*, vol. 11, no. 2, pp. 7018–7022, Apr. 2021, https://doi.org/10.48084/etasr.4104.

[22] O. Cristea, N.-S. Popa, M.-G. Manea, and C. Popa, "About the Automation of an Autonomous Sail-propelled Search Drone," *Engineering, Technology & Applied Science Research*, vol. 13, no. 6, pp. 12334–12341, Dec. 2023, https://doi.org/10.48084/etasr.6502.

[23] C. Tian, J. Wang, Z. Yin, and G. Yu, "Integral backstepping based nonlinear control for quadrotor," in *35th Chinese Control Conference*, Chengdu, China, Jul. 2016, pp. 10581–10585, https://doi.org/10.1109/ChiCC.2016.7555034.

[24] A. Poultney, P. Gong, and H. Ashrafiuon, "Integral backstepping control for trajectory and yaw motion tracking of quadrotors," *Robotica*, vol. 37, no. 2, pp. 300–320, Feb. 2019, https://doi.org/10.1017/S0263574718001029.

[25] S.-H. Tsai, Y.-P. Chang, H.-Y. Lin, and L.-M. Chang, "Design and Implementation of Integral Backstepping Sliding Mode Control for Quadrotor Trajectory Tracking," *Processes*, vol. 9, no. 11, Nov. 2021, Art. no. 1951, https://doi.org/10.3390/pr9111951.

[26] D. J. Almakhles, "Robust Backstepping Sliding Mode Control for a Quadrotor Trajectory Tracking Application," *IEEE Access*, vol. 8, pp. 5515–5525, Jan. 2020, https://doi.org/10.1109/ACCESS.2019.2962722.

[27] S. Ullah, Q. Khan, A. Mehmood, and R. Akmeliawati, "Integral backstepping integral sliding mode control of underactuated nonlinear electromechanical systems," *Control Engineering and Applied Informatics*, vol. 21, no. 3, pp. 42–50, Sep. 2019.

[28] F. Chen, R. Jiang, K. Zhang, B. Jiang, and G. Tao, "Robust Backstepping Sliding-Mode Control and Observer-Based Fault Estimation for a Quadrotor UAV," *IEEE Transactions on Industrial Electronics*, vol. 63, no. 8, pp. 5044–5056, Aug. 2016, https://doi.org/10.1109/TIE.2016.2552151.

[29] Z. Jia, J. Yu, Y. Mei, Y. Chen, Y. Shen, and X. Ai, "Integral backstepping sliding mode control for quadrotor helicopter under external uncertain disturbances," *Aerospace Science and Technology*, vol. 68, pp. 299–307, Sep. 2017, https://doi.org/10.1016/j.ast.2017.05.022.

[30] X. Dang, X. Zhao, C. Dang, H. Jiang, X. Wu, and L. Zha, "Incomplete differentiation-based improved adaptive backstepping integral sliding mode control for position control of hydraulic system," *ISA Transactions*, vol. 109, pp. 199–217, Mar. 2021, https://doi.org/10.1016/j.isatra.2020.10.027.

[31] N. Dalwadi, D. Deb, and S. M. Muyeen, "Adaptive backstepping controller design of quadrotor biplane for payload delivery," *IET Intelligent Transport Systems*, vol. 16, no. 12, pp. 1738–1752, 2022, https://doi.org/10.1049/itr2.12171.

[32] S. H. Derrouaoui, Y. Bouzid, and M. Guiatni, "Adaptive integral backstepping control of a reconfigurable quadrotor with variable parameters' estimation," *Proceedings of the Institution of Mechanical Engineers, Part I: Journal of Systems and Control Engineering*, vol. 236, no. 7, pp. 1294–1309, Aug. 2022, https://doi.org/10.1177/09596518221087803.

[33] K. Eliker and W. Zhang, "Finite-time Adaptive Integral Backstepping Fast Terminal Sliding Mode Control Application on Quadrotor UAV," *International Journal of Control, Automation and Systems*, vol. 18, no. 2, pp. 415–430, Feb. 2020, https://doi.org/10.1007/s12555-019-0116-3.